Functional Annotation and Kinetic Characterization of PhnO from *Salmonella enterica*†

James C. Errey and John S. Blanchard*

Department of Biochemistry, Albert Einstein College of Medicine, 1300 Morris Park Avenue, Bronx, New York 10461

Received November 9, 2005; Revised Manuscript Received January 9, 2006

ABSTRACT: Phosphorus is an essential nutrient for all living organisms. Under conditions of inorganic phosphate starvation, genes from the Pho regulon are induced, allowing microorganisms to use phosphonates as a source of phosphorus. The *phnO* gene was previously annotated as a transcriptional regulator of unknown function due to sequence homology with members of the GCN5-related *N*-acyltransferase family (GNAT). PhnO can now be functionally annotated as an aminoalkylphosphonic acid *N*-acetyltransferase which is able to acetylate a range of aminoalkylphosphonic acids. Studies revealed that PhnO proceeds via an ordered, sequential kinetic mechanism with AcCoA binding first followed by aminoalkylphosphonate. Attack by the amine on the thioester of AcCoA generates the tetrahedral intermediate that collapses to generate the products. The enzyme also requires a divalent metal ion for activity, which is the first example of this requirement for a GNAT family member.

Phosphorus plays an essential role in the physiology and biochemistry of all living organisms. It is therefore not surprising that microorganisms have evolved sophisticated systems to acquire phosphorus from sources other than inorganic orthophosphate. Under phosphate starvation conditions, when other more readily utilizable forms of phosphate are not present, microorganisms have evolved to utilize more reduced organophosphorus sources, including phosphonates (*1*). Phosphonates are a class of compounds which contain a carbon−phosphorus (C−P) bond that is exceptionally stable and resistant to chemical hydrolysis, thermal decomposition, and photolysis (*2*). Phosphonates are a naturally occurring class of compounds which are present in a number of organisms; e.g., *Tetrahymena* which possesses up to 30% of its membrane lipids in the form of phosphonolipids (*3*).

Changing the source of phosphorus from orthophosphate to organophosphorus compounds is a tightly regulated process. Under phosphate starvation conditions, genes from the Pho (phosphate starvation) regulon are induced (*1*). In Gram-negative organisms, such as *Salmonella enterica* serovar *typhimurium*, the *pho* genes are regulated by a two-component system, which consists of PhoB and PhoR; PhoB binds directly to the *pho* gene promoter while PhoR is a P_i sensory histidine protein kinase (*4*). Two alternative pathways exist for cleavage of the C−P bond: the C−P lyase and the phosphonatase pathways (Scheme 1 (*5*). *Escherichia coli* carries genes for the reductive C−P lyase pathway (*6*), while *S. enterica* carries genes for the phosphonatase pathway (*7*). The C−P lyase pathway has a much broader substrate specificity and is able to cleave alkylphosphonates as well as aminoalkylphosphonates (*8*, *9*). In comparison, the phosphonatase pathway has much narrower substrate specificity and acts only on 2-aminoethylphosphonate (*10*). Mutagenic studies and sequence analysis of the Pho regulon in *E. coli* identified a number of genes involved in phosphonate catabolism designated *phnC* to *phnP* (*11*, *12*). PhnC, PhnD, and PhnE were proposed to constitute a phosphonate transporter while PhnG, PhnH, PhnI, PhnJ, PhnK, PhnL, and PhnM were required for catalysis and were proposed to form a membrane-associated carbon−phosphorus (C−P) lyase. PhnN and PhnP were not absolutely required for phosphonate catabolism and were therefore proposed to be accessory proteins for the C−P lyase. PhnF and PhnO were nonessential and were proposed to play regulatory roles because of sequence similarities to other regulatory proteins (*11*).

Scheme 1: Pathways for Phosphonate Catabolism[a]

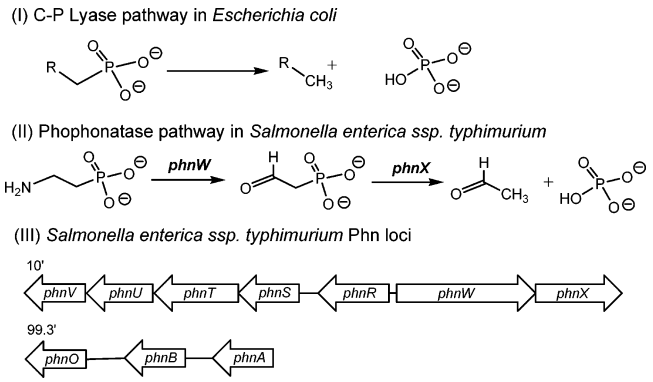

[a] (I) The C−P lyase pathway acts on alkylphosphonates as well as aminoalkylphosphonates. (II) The phosphonatase pathway that uses 2-aminoethylphosphonate and cleaves the C−P bond in a two-step transamination and hydrolysis process. (III) The *S. enterica phn* gene locus; *phnR* encodes a putative aminoalkylphosphonate transport repressor, *phnS*−*V* encode putative aminoalkylphosphonate transport components, *phnW* encodes a 2-aminoethylphosphonate transaminase, *phnX* encodes a 2-phosphonoacetaldehyde hydrolase, *phnA* encodes a putative phosphonoacetate hydrolase, *phnB* encodes a putative phosphonoacetate transporter, and *phnO* encodes an aminoalkylphosphonic *N*-acetyltransferase.

† This work was supported by NIH Grants AI33696 and AI60899.

* Corresponding author. Tel: (718) 430-3096. Fax: (718) 430-8565. E-mail: blanchar@aecom.yu.edu.

10.1021/bi052297p CCC: $33.50
Published on Web 02/08/2006

In contrast to the *E. coli* Pho regulon, which consists of at least 31 coregulated genes, the *S. enterica* Pho regulon is smaller, consisting of only 21 genes (*7*). The *S. enterica* Phn locus differs from the *E. coli* Phn locus in its size, layout, and composition, primarily due to their differing mechanisms of phosphonate catabolism. The *S. enterica* Phn locus is composed of seven genes, designated *phnR* to *phnX*, although another cluster containing three genes designated *phnA*, *phnB*, and *phnO* is putatively involved in phosphonate catabolism (Scheme 1) (*7*, *13*). Unlike the C−P lyase pathway, the phosphonatase pathway has been extensively mechanistically characterized (*7*, *10*, *14*, *15*). The initial step in the catabolism of 2-aminoethylphosphonate in *S. enterica* is a PLP-dependent transamination, carried out by 2-aminoethylphosphonate transaminase (the *phnW* gene product) (*10*). This is followed by a metal-dependent hydrolysis of the C−P bond catalyzed by 2-phosphonoacetaldehyde hydrolase (the *phnX* gene product) (*16*, *17*). Interestingly, the *phnO* gene is present in both *E. coli* and *S. enterica*, even though they have very different mechanisms of phosphonate catabolism (*6*, *7*). Gene knockout studies have shown that the *E. coli phnO* gene product was not required for the catabolism of phosphonates and was presumed to play a regulatory role (*11*). Furthermore, *phnO* showed significant sequence homology to the GCN5-related *N*-acetyltransferases family (GNAT),[1] of which some members such as the histone acetyltransferases play a regulatory role (*18*).

In this paper, we describe the cloning, expression, and purification of PhnO from *S. enterica* serovar *typhimurium* LT2 and define its functionality as an aminoalkylphosphonic acid *N*-acetyltransferase. We have determined the steady-state kinetic parameters, defined the divalent metal ion dependency, and explored the steady-state kinetic mechanism. General acid catalysis is used by the enzyme, and this is likely to be the rate-limiting step as assessed by solvent deuterium kinetic isotope effects.

MATERIALS AND METHODS

All chemicals, acetyl-coenzyme A (AcCoA), and aminoalkylphosphonic acids were purchased from Sigma-Aldrich Chemical Co. or Fisher Scientific. pET-17b(−) plasmid was purchased from Novagen. All restriction enzymes and T4 DNA ligase were obtained from New England Biolabs. *E. coli* strain BL21(DE3) star cells, PCR primers, and the pCR-Blunt plasmid kit were obtained from Invitrogen. *Pfu* DNA polymerase was purchased from Stratagene. Desulfo-CoA was synthesized as previously described (*19*). All divalent metals used in this study were prepared from their respective chloride salt.

General Methods. Solution pH values were measured at 25 °C with an Accumet model 20 pH meter and Accumet combination electrode standardized at pH 7.0 and 4.0 or 10.0. Protein purification was performed at 4 °C using a fast protein liquid chromatography system (Amersham-Pharmacia Biotech). Spectrophotometric assays were performed using a UVIKON XL double beam UV−vis spectrophotometer (BIO-TEK Instruments). All buffers were passed through Chelex 100 resin (Bio-Rad) to remove any divalent metal ions present.

Cloning, Expression, and Purification of PhnO. The *S. enterica* serovar *typhimurium* LT2 gene *phnO* was amplified by PCR using the primers 5-TTTTTCATATGCCAGTCT-GTGAATTACGCCA-3 and 5-TTTTTTGAATTCTCACA-ATGCTTTCGTAAACC-3 from the plasmid template pET-28a(−):*phnO* (generously provided by Sophie Magnet, Albert Einstein College of Medicine), incorporating *Nde*I and *Eco*RI restriction endonuclease sites (underlined). The amplified DNA product was ligated into a pCR-−Blunt plasmid and transformed into One Shot TOP10 cells. Plasmid DNA isolated from these cells was then digested with *Nde*I and *Eco*RI, and the purified insert was ligated into purified plasmid pET-17b(−) previously linearized with the same restriction enzymes, yielding an expression plasmid for *S. enterica phnO*.

The plasmid pET-17b(−):*phnO* was then isolated, sequenced, and used to transform *E. coli* BL21(DE3) star cells. Transformed cells were grown overnight in 50 mL of LB broth containing 100 μg/mL ampicillin. One liter cultures were then inoculated, and the cells were grown at 37 °C to an A_{600} of 0.8. Cells were then induced by the addition of 0.5 mM isopropyl β-D-thiogalactopyranoside (IPTG) and left to grow for a further 16 h at 37 °C. Soluble expression of the protein was confirmed by sodium dodecyl sulfate−polyacrylamide gel electrophoresis (SDS−PAGE).

All protein purification steps were carried out at 4 °C. The cell pellet (30 g) was resuspended in 50 mL of buffer A (buffer A: 20 mM CHES, pH 8.75), containing two tablets of Complete protease inhibitor cocktail (Roche). The cells were disrupted on ice by sonication using a Branson sonifier 450. The suspension was then centrifuged (10000*g* for 30 min) to remove cell debris. The supernatant was filtered using a 0.2 μm Millipore syringe filter and applied to a 140 mL fast-flow Q-Sepharose anion-exchange column preequilibrated with buffer A. The proteins were eluted with a linear, 1 L gradient of NaCl (0−1 M NaCl) in buffer A volumes at 1 mL/min. Protein was detected with an on-line detector monitoring A_{280}, and column fractions were collected and analyzed by SDS−PAGE. Fractions containing the ca. 16 kDa protein were pooled, and $(NH_4)_2SO_4$ was added to a final concentration of 1.5 M. After centrifugation to remove insoluble material, the supernatant was applied to a 140 mL phenyl-Sepharose column preequilibrated with buffer C [20 mM CHES, pH 8.75, 1.5 M $(NH_4)_2SO_4$]. Proteins were eluted with a linear, 1 L 1.5−0 M $(NH_4)_2SO_4$ gradient at 1 mL/min. The active fractions were pooled and dialyzed extensively against buffer A. The sample was then applied to a 25 mL Mono-Q column anion-exchange column preequilibrated with buffer A, and proteins were eluted with a linear 750 mL gradient of NaCl (0−1 M NaCl) in buffer A at 1 mL/min. The active fractions were pooled and dialyzed four times against 4 L of buffer D [buffer D: 20 mM HEPES, 10 mM EDTA, 100 mM $(NH_4)_2SO_4$, pH 8.25], concentrated using a YM10 Amicon ultrafiltration membrane to a final concentration of 20 mg/mL, and stored in 50% glycerol at −20 °C.

[1] Abbreviations: AcCoA, acetyl-coenzyme A; CHES, 2-(cyclohexylamino)ethanesulfonic acid; CoA, coenzyme A; DTDP, 4,4′-dithiodipyridine; EDTA, (ethylenedinitrilo)tetraacetic acid; GNAT, GCN5-related *N*-acyltransferase; HEPES, *N*-(2-hydroxyethyl)piperazine-*N*′-2-ethanesulfonic acid; IPTG, isopropyl β-D-thiogalactopyranoside; LB, Luria broth; PCR, polymerase chain reaction; PIPES, piperazine-1,4-bis(2-ethanesulfonic acid); *S*-1AEP, (*S*)-1-aminoethylphosphonic acid; SDS−PAGE, sodium dodecyl sulfate−polyacrylamide gel electrophoresis; TEA, triethanolamine.

Determination of Protein Concentration. The enzyme concentration was determined from $\epsilon_{280nm} = 17780\ M^{-1}\ cm^{-1}$ for native PhnO, and turnover numbers are based on an enzyme monomer. The concentration of enzyme was also determined using the bicinchoninic acid protein assay (Pierce) with bovine serum albumin as a standard, which agreed favorably with the value obtained by A_{280}.

Measurement of Enzyme Activity. Initial velocities for the reaction of PhnO were determined using 4,4′-dithiodipyridine (DTDP) to continuously detect the formation of the product CoA at 324 nm (thiopyridone: $\epsilon = 19800\ M^{-1}\ cm^{-1}$) at 25 °C. A typical reaction mix contained 100 mM HEPES, pH 7.5, 100 mM $(NH_4)_2SO_4$, 200 μM DTDP, 1 mM AcCoA, and 2 mM aminoalkylphosphonate in a final volume of 1 mL. Reactions were initiated by the addition of enzyme, typically 2 nM final concentration. Ni^{2+} (100 μM) was typically included because a divalent metal is essential for activity.

Initial Velocity Experiments. Initial velocity kinetic data were fitted using Sigma Plot 2000. The substrate specificity of PhnO was determined at pH 7.5 at 10 different concentrations of the variable substrate and a fixed, saturating concentration of the second substrate and at saturating concentrations of Ni^{2+} (100 μM). Kinetic constants for AcCoA and other CoA derivatives were determined at fixed, saturating concentrations of (*S*)-1-aminoethylphosphonic acid (*S*-1AEP) (3 mM) and Ni^{2+}, while kinetic constants for the aminoalkylphosphonates were determined using fixed, saturating concentrations of AcCoA (1 mM) and Ni^{2+}. Kinetic constants for divalent metal ions were determined at fixed, saturating concentrations of *S*-1AEP and AcCoA. Individual substrate saturation kinetic data were fitted to the equation:

$$v = VA/(A + K) \quad (1)$$

where V is the maximal velocity, A is the substrate concentration, and K is the Michaelis−Menten constant (K_m). Initial velocity patterns were obtained by measuring the initial rate at five concentrations of each substrate. Equation 2 was used to fit the intersecting initial velocity pattern:

$$v = VAB/(K_{ia}K_B + K_aB + K_BA + AB) \quad (2)$$

where A and B are the concentrations of the substrates, K_A and K_B are the Michaelis−Menten constants for the substrates, and K_{ia} is the inhibition constant for substrate A.

Dead-End Inhibition Studies. Dead-end inhibition patterns were determined by measuring initial velocities (<10% completion) at variable concentrations of one reactant, the second reactant concentration fixed at its K_m value, a fixed, saturating concentration of Ni^{2+}, and the inhibitor at several concentrations. Equations 3 and 4 were used to fit linear, competitive and linear, noncompetitive inhibition data, respectively:

$$v = VA/[K(1 + I/K_{is}) + A] \quad (3)$$

$$v = VA/[K(1 + I/K_{is}) + A(1 + I/K_{ii})] \quad (4)$$

where I is the inhibitor concentration and K_{is} and K_{ii} are the slope and intercept inhibition constants, respectively.

Dependence of PhnO Activity on pH. The pH dependence of the kinetic parameters exhibited by PhnO were determined using *S*-1AEP as the variable substrate. Acetyltransferase activity was monitored from pH 6.75 to pH 8.5 every ~0.5 pH unit using the following buffers: PIPES (pH 6.75−7.35) and HEPES (pH 7.15−8.5). The resulting kinetic data were fitted to eq 1 to obtain the kinetic parameters k_{cat} and k_{cat}/K_m. Profiles were generated by plotting the log of k_{cat} or k_{cat}/K_m versus the pH and fitted using the equations:

$$\log y = \log C/(1 + H/K) \quad (5)$$

$$\log y = \log C/(1 + H^2/K^2) \quad (6)$$

where y is k_{cat} or k_{cat}/K_m, C is the pH-independent value of k_{cat} or k_{cat}/K_m, H is $[H^+]$, and K represents the observed dissociation constant(s) for the ionizing group(s).

Solvent Kinetic Isotope Effects. The solvent kinetic isotope effects on k_{cat} and k_{cat}/K_m were determined by measuring the initial velocities using saturating concentrations of AcCoA and Ni^{2+} while varying the concentration of *S*-1AEP in either H_2O or 90% D_2O at pH 8.15. Solvent deuterium kinetic isotope effects were fitted to the equation

$$v = VA/[KA(1 + F_iE_{V/K}) + A(1 + F_iE_V)] \quad (7)$$

where $E_{V/K}$ and E_V are the isotope effects on $k_{cat}/K_m - 1$ and $k_{cat} - 1$, respectively, and F_i represents the fraction of isotope.

RESULTS AND DISCUSSION

Cloning, Expression, and Purification of PhnO. To obtain large quantities of PhnO for mechanistic studies, the *phnO* gene was cloned into plasmid pET-17b(−) and expressed in *E. coli* BL21(DE3) star cells. PhnO was purified using a combination of anion exchange/hydrophobic interaction column chromatographies. These methods were sufficient to achieve a catalytically active protein that was greater than 95% homogeneous (as judged by SDS−PAGE). Approximately 200 mg of purified enzyme was obtained from 30 g of cell paste. Protein electrospray ionization−mass spectrometry was performed on the purified protein, revealing a single species with a molecular mass of 16499 Da, compared to 16632 Da expected for full-length PhnO, indicating that the N-terminal *N*-formylmethionine has been posttranslationally removed. Dynamic light scattering was performed on the protein sample revealing that the protein existed as a dimer (data not shown).

Substrate Specificity of PhnO. The substrate specificity of *S. enterica* PhnO for acyl-CoA derivatives, summarized in Table 1, was determined at fixed saturating concentrations of *S*-1AEP and Ni^{2+}. On the basis of k_{cat}/K_m values and the probability that AcCoA was the likely physiologically relevant substrate, AcCoA was used as the acyl donor in all subsequent experiments. The kinetic parameters of various aminoalkylphosphonic acids determined at fixed saturating concentrations of AcCoA and Ni^{2+} are also summarized in Table 1. The kinetic behavior of the aminoalkylphosphonic acid followed two clear patterns. Increasing the alkyl chain from ethyl to butyl resulted in approximately a 70-fold increase in the K_m values and 13-fold decrease in k_{cat} values, indicating a preference for shorter aminoalkylphosphonic acids. The kinetic data also suggested that the position of the amine group was important with a preference for the 1 position. The k_{cat}/K_m value for *S*-1AEP was 15-fold higher

Table 1: Kinetic Parameters for PhnO with Various Acyl-CoAs and Aminoalkylphosphonates

compound	K_m (mM)	k_{cat} (s^{-1})	k_{cat}/K_m (M^{-1} s^{-1})
acetyl-CoA[a]	0.06 ± 0.01	13.1 ± 0.1	(2.2 ± 0.3) × 10^5
propionyl-CoA[a]	0.07 ± 0.01	14.7 ± 0.7	(2.1 ± 0.3) × 10^5
malonyl-CoA[a]	0.05 ± 0.01	0.4 ± 0.1	(8.0 ± 0.6) × 10^3
aminomethylphosphonic acid[b]	1.7 ± 0.1	7.0 ± 0.1	(4.1 ± 0.2) × 10^3
2-aminoethylphosphonic acid[b]	1.8 ± 0.1	9.0 ± 0.2	(5.0 ± 0.2) × 10^3
3-aminopropylphosphonic acid[b]	4.0 ± 0.4	5.4 ± 0.1	(1.4 ± 0.1) × 10^3
4-aminobutylphosphonic acid[b]	13.0 ± 1.0	0.5 ± 0.1	(3.8 ± 0.4) × 10^1
(*S*)-1-aminoethylphosphonic acid[b]	0.17 ± 0.01	13.3 ± 0.1	(7.8 ± 0.4) × 10^4
(*R*)-1-aminoethylphosphonic acid[b]	NS[c]		
1-aminopropylphosphonic acid[b]	4.1 ± 0.2	7.4 ± 0.1	(1.8 ± 0.1) × 10^3
1-aminobutylphosphonic acid[b]	12.5 ± 0.8	1 ± 0.1	(8.0 ± 0.5) × 10^1
D-alanine[b]			(3.0 ± 0.3) × 10^1
2-aminoethanesulfonic acid[b]	18.9 ± 0.9	14.8 ± 0.2	(7.8 ± 0.3) × 10^2
2-aminoethanesulfinic acid[b]	16.4 ± 0.7	20 ± 0.3	(1.2 ± 0.1) × 10^3

[a] Values for acyl-CoA's were determined at a fixed, saturating concentration of (*S*)-1-aminoethylphosphonic acid. [b] Values for aminoalkylphosphonates, and analogues, were determined at a fixed, saturating concentration of AcCoA. [c] NS: not a substrate.

than 2-aminoethylphosphonic acid, primarily being an effect on the K_m value. The selectivity for the phosphonic acid group was also investigated. Replacement with a carboxyl group, yielding D-alanine, yielded a very poor substrate for which saturation could not be obtained. For D-alanine, only an observed k_{cat}/K_m of 3.0 × 10^1 M^{-1} s^{-1} could be calculated, some 2600-fold lower than the k_{cat}/K_m observed for *S*-1AEP. Mimics of the phosphonate group were also investigated with aminoalkylsulfinic (SO_2H) and aminoalkylsulfonic (SO_3H) acids. An approximate 5-fold decrease of k_{cat}/K_m values was observed with respect to their corresponding phosphonic acid (2-aminoethylphosphonic acid) values, and this is primarily a K_m effect.

Metal Ion Requirments. Various divalent metal ions were examined as activators for PhnO. Other enzymes involved in phosphonate catabolism have shown a metal ion dependency, most notably 2-phosphonoacetaldehyde hydrolase (phosphonatase), which requires magnesium for coordination of the phosphonate (*17*). To investigate whether a tightly bound metal ion was playing a similar role to that observed in phosphonatase, following the final Mono-Q column, PhnO was dialyzed extensively against buffer D in the presence and absence of 10 mM EDTA. Following dialysis with EDTA, PhnO was assayed in the absence of any divalent metal ions. The observed k_{cat}/K_m for *S*-1AEP decreased dramatically after EDTA treatment to 7.2 × 10^2 M^{-1} s^{-1}, this being primarily being a K_m effect (Table 2). In contrast when PhnO was extensively dialyzed against buffer alone, the observed k_{cat}/K_m value was 4.6 × 10^4 M^{-1} s^{-1}, or half the value determined in the presence of saturating divalent metal ion. This suggests that the enzyme retains half an equivalent of tightly bound divalent metal ion throughout the purification. The metal ion specificity of EDTA-treated PhnO was examined as a function of both the metal ion at fixed, saturating concentrations of AcCoA and *S*-1AEP and the amino phosphonate at fixed concentrations of AcCoA and divalent metal ions (Table 2). The resulting hyperbolic curves (data not shown) were fitted to eq 1 to obtain maximal k_{cat} and K_m values and, in the case of the metal ions, the parameter K_{act}, which is defined as the concentration of divalent metal ion required to half-saturate the rate. The *S. enterica* PhnO exhibited a preference for Ni^{2+} followed by Mn^{2+} and very poor activity with Mg^{2+}, as evaluated by the k_{cat}/K_{act} values; however, it is unclear what the physiologically relevant metal ion activator is, and further studies are required.

Table 2: Kinetic Parameters for PhnO with Various Divalent Metal Ions

	$K_{m,S-1AEP}$ (mM)	k_{cat} (s^{-1})	k_{cat}/K_m (M^{-1} s^{-1})
Mn^{2+} [a]	0.30 ± 0.02	20.6 ± 0.2	(6.9 ± 0.4) × 10^4
Ni^{2+} [a]	0.17 ± 0.01	13.1 ± 0.1	(8.1 ± 0.3) × 10^4
Co^{2+} [a]	0.28 ± 0.06	10.0 ± 0.4	(3.6 ± 0.7) × 10^4
Mg^{2+} [a]	2.00 ± 0.06	17.0 ± 0.3	(8.5 ± 0.3) × 10^3
EDTA treated[a]	18.00 ± 0.76	13.0 ± 0.3	(7.2 ± 0.3) × 10^2
non EDTA treated[a]	0.20 ± 0.02	9.2 ± 0.2	(4.6 ± 0.4) × 10^4

	K_{act} (μM)	k_{cat} (s^{-1})	k_{cat}/K_{act} (M^{-1} s^{-1})
Mn^{2+} [b]	6.8 ± 0.6	18.7 ± 1.1	(2.7 ± 0.3) × 10^6
Ni^{2+} [b]	0.6 ± 0.1	13.0 ± 0.3	(2.2 ± 0.3) × 10^7
Co^{2+} [b]	1.3 ± 0.4	8.9 ± 1.1	(6.8 ± 2.2) × 10^6
Cu^{2+} [b]	15.9 ± 2.4	4.5 ± 0.2	(2.8 ± 0.4) × 10^5
Mg^{2+} [b]	850 ± 63	16.8 ± 0.2	(2.0 ± 0.1) × 10^4

[a] Kinetic parameters for *S*-1AEP were determined at a fixed, saturating concentration of AcCoA and the indicated metal ion. [b] Kinetic parameters for divalent metal ion activation at saturating concentrations of *S*-1AEP and AcCoA.

Kinetic Mechanism. Reactions catalyzed by GNAT acetyltransferases are known to proceed through two distinct mechanisms (*18*). Only the ESA1 histone acetyltransferase has been shown to proceed via a ping-pong mechanism, with the transfer of the acetyl group from AcCoA to a cysteinyl residue of the enzyme and the subsequent transfer to the ϵ-amino group of the histone lysine residue (*20*). The other is a sequential mechanism, where a ternary complex of enzyme, AcCoA, and substrate forms and the acetyl group of AcCoA is directly transferred to a substrate. Reactions catalyzed by all other GNAT superfamily members studied so far proceed through such a sequential kinetic mechanism (*18*). The initial velocity patterns were determined using *S*-1AEP and AcCoA at five different concentrations, respectively, and at a fixed, saturating concentration of Ni^{2+}. The resultant double-reciprocal plot was intersecting, diagnostic of a sequential kinetic mechanism in which both substrates must bind to the enzyme before chemistry can take place (Figure 1). Dead-end inhibition experiments were carried out using desulfo-coenzyme A versus either AcCoA or *S*-1AEP. Desulfo-coenzyme A is a coenzyme A analogue that lacks the terminal sulfhydryl of CoA and is a dead-end inhibitor

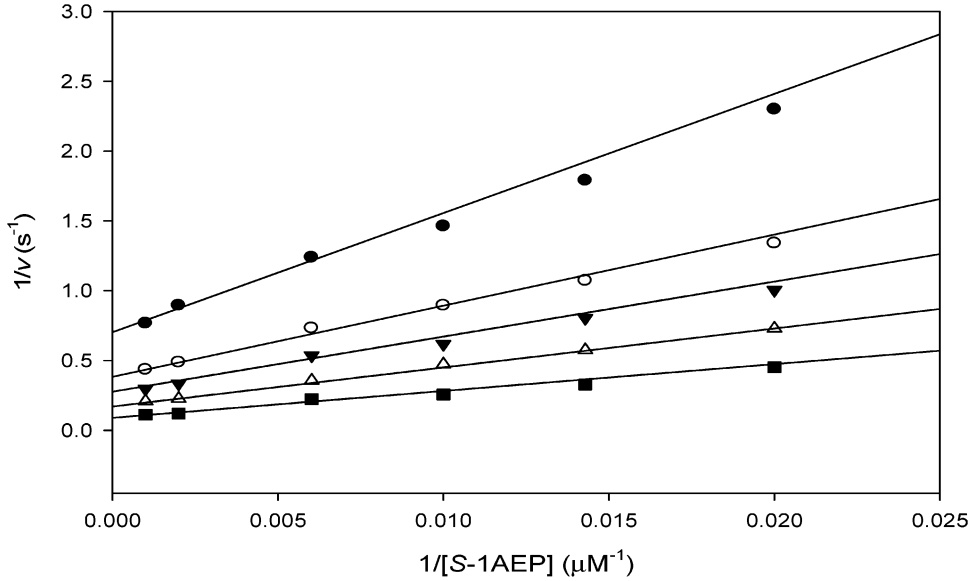

FIGURE 1: Double reciprocal plot of initial rate data at varying *S*-1AEP concentrations and fixed concentrations of AcCoA at 10 μM (●), 20 μM (○), 30 μM (▼), 60 μM (△), and 250 μM (■). The pattern of intersecting lines is indicative of a sequential kinetic mechanism.

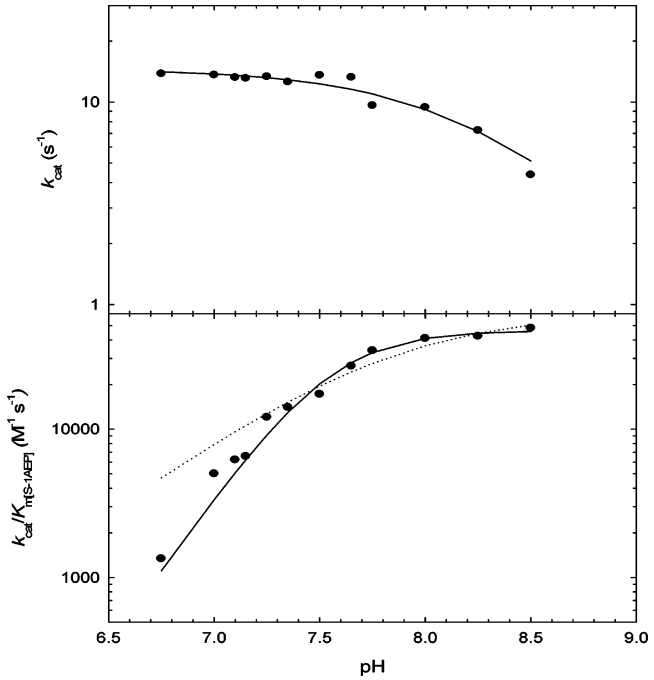

FIGURE 2: Dependence of k_{cat} and k_{cat}/K_{S-1AEP} on pH at saturating levels of AcCoA and Ni^{2+}. The dotted and solid lines are fits to eqs 5 and 6, respectively. The k_{cat} pH profile revealed the presence a single ionizable group with a p*K* value of 8.2 (±0.1). The k_{cat}/K_{S-1AEP} profile was fit to eq 6, which describes the dependence on two groups with similar p*K* values of 7.5 (±0.1) and eq 5, which describes the dependence on one group (dotted line).

since it forms a nonproductive complex with PhnO and the aminophosphonic acid. Desulfo-coenzyme A exhibited linear, competitive inhibition versus AcCoA (K_{is} = 79 ± 3 μM) and linear, noncompetitive inhibition versus S-1AEP (K_{is} = 219 ± 44 μM; K_{ii} = 204 ± 33 μM). These dead-end inhibition patterns are only compatible with the ordered binding of AcCoA followed by *S*-1AEP, as has been observed with other GNAT acetyltransferases (*18*).

Dependence of pH. pH studies were performed to investigate the ionization behavior of groups responsible for catalysis and binding. The pH dependency of k_{cat} and $k_{cat}/K_{m,S-1AEP}$ was investigated at saturating concentrations of

Scheme 2: Proposed Kinetic and Chemical Mechanisms for Aminophosphonate N-Acetylation by PhnO

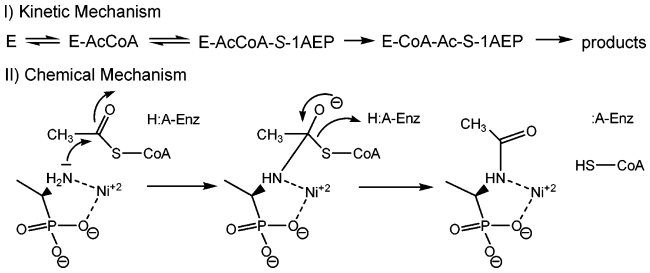

AcCoA and Ni^{2+}. The k_{cat} pH profile revealed the presence a single ionizable group exhibiting a p*K* value of 8.2 (±0.1). We ascribed this group to an enzymic group that functions as a general acid involved in protonation of the initially formed thiolate after tetrahedral intermediate collapse. The $k_{cat}/K_{m,S-1AEP}$ profile reveals two groups with similar p*K* values of 7.5 (±0.1) (Figure 2). The two similar pK_a's are likely to be ionizable groups from the aminoalkylphosphonate substrate, most likely the amine and the phosphonoxygen groups [both have pK_a values around 7 (*21*)], both of which are unprotonated when *S*-1AEP binds to the E−AcCoA complex. From these data a chemical mechanism can be proposed where, after ordered substrate binding, a tetrahedral intermediate is formed followed by intermediate collapse and protonation of the CoA thiolate (Scheme 2). The exact role of the metal ion is unclear but could bind to the enzyme and aid in the binding of the aminoalkylphosphonate by coordinating the oxygens of the phosphonate group in a fashion similar to which 2-phosphonoacetaldehyde hydrolase binds to Mg^{2+} (*17*). However, we favor a role in which the metal binds to the enzyme and the aminoalkylphosphonate contributes both the amine and one of the phosphonoxygens atoms as metal ligands, which is supported by the absence of any *general* base catalysis observed in the k_{cat} pH profile. Preliminary isothermal titration calorimetry data suggest that metals can bind to the free enzyme (data not shown). This could position the amine group of the aminoalkylphosphonate for acetyl transfer and reduce the p*K* of the amine, making it more nucleophilic for attack on the thioester [such metal

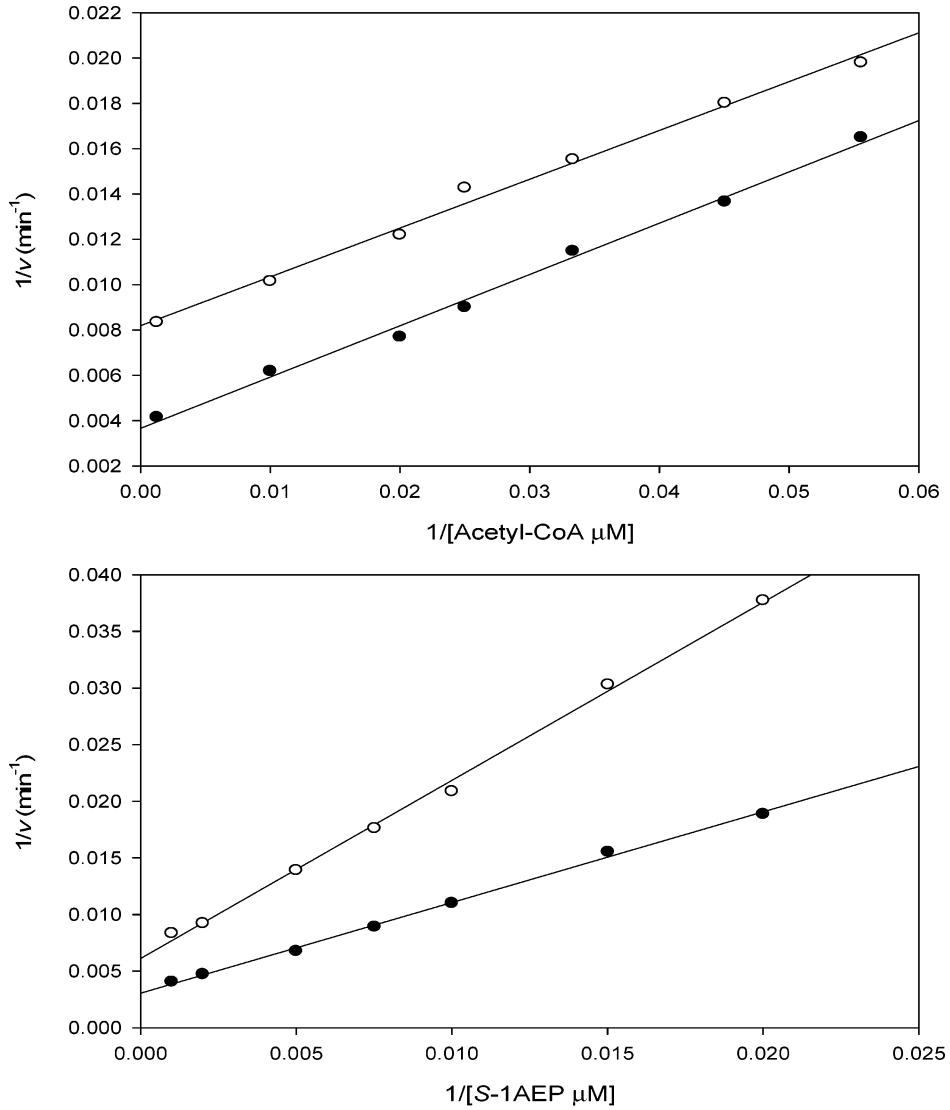

FIGURE 3: Reciprocal plots of the solvent kinetic isotope effect determined for PhnO using AcCoA (top panel) or *S*-1AEP (bottom panel) as the variable substrate in the presence of saturating concentrations of Ni^{2+}. The symbols are the experimentally determined values in H_2O (●) or 90% D_2O (○), while the lines are fits of the data to eq 7.

complexes of aminoalkylphosphonates have previous been described (*22*)].

Solvent Kinetic Isotope Effects. Solvent kinetic isotope effects were determined by measuring initial velocities in both H_2O and 90% D_2O. Both AcCoA and *S*-1AEP were investigated as the variable substrate at seven different concentrations, with reactions performed under fixed, saturating concentrations of the other substrate and Ni^{2+}. These experiments were performed at pH 8.15 where both k_{cat} and k_{cat}/K_m are relatively independent of pH. When AcCoA was the variable substrate, a $^{D_2O}k_{cat}/K_{AcCoA}$ value of unity and a $^{D_2O}k_{cat}$ value of 2.2 (±0.1) were observed, implying that AcCoA binds first, and its dissociation is prevented by *S*-1AEP binding. When *S*-1AEP was the variable substrate, equivalent solvent kinetic isotope effects of 2.2 (±0.1) were observed on $^{D_2O}k_{cat}$ and $^{D_2O}k_{cat}/K_{S-1AEP}$, suggesting that *S*-1AEP is not a "sticky substrate" (Figure 3). These data are in agreement with the dead-end studies that suggested an ordered binding of AcCoA followed by the aminoalkylphosphonate.

A proton inventory experiment was performed by varying the atom fraction of D_2O at saturating concentrations of both *S*-1AEP and AcCoA using Ni^{2+} as the metal activator. Each data point was determined in triplicate, yielding a linear relation between the rate and mole fraction of deuterium (data not shown). The equivalent values of $^{D_2O}k_{cat}$ and $^{D_2O}k_{cat}/K_{S-1AEP}$ and the linear proton inventory suggest that a single proton is transferred in a step that is at least partially rate-limiting in the chemical reaction catalyzed by PhnO. On the basis of the k_{cat} pH profile, the most likely single proton transfer is from the enzymic general acid to the thiolate of CoA, formed upon decomposition of the tetrahedral intermediate. In the structures of a number of GNAT−substrate complexes, a suitably positioned tyrosine residue has been ascribed as the general acid (*18*).

CONCLUDING REMARKS

Although we have demonstrated that PhnO functions as an aminoalkylphosphonic *N*-acetyltransferase, a number of questions still exist. PhnO acetylates a range of aminoalkylphosphonates, including the physiologically relevant 2-aminoethylphosphonic acid. The chemical and kinetic mechanisms proposed are similar to those proposed for other GNAT acetyltransferases, with the sequential binding of AcCoA

followed by the binding of the acyl acceptor (the aminoalkylphosphonate), with subsequent formation of the tetrahedral intermediate and product release (*23*). However, the divalent metal ion activation that was observed is, to date, unique for a GNAT acetyltransferase. It seems likely that the divalent metal ion activation has evolved to play a specific role in aminoalkylphosphonate binding similar to that observed in other enzymes involved in phosphonate catabolism (phosphonatase) (*17*). This would also serve to reduce the p*K* value of the amine and assist in catalysis. The physiological relevance of the PhnO-catalyzed reaction is unclear, as acetylation of the amine group would prevent its transamination and subsequent cleavage of the C−P bond. We propose two physiological roles for aminoalkylphosphonate acetylation: storage and protection. When amounts of aminoalkylphosphonates are available in the environment that exceed the organism's phosphate requirements, these phosphonates can be stored in an acetylated form and later used after hydrolysis by a deacetylase. *S*-1AEP is known to have antibacterial properties (*24*). *S*-1AEP is a structural analogue of D-alanine, a component of the muramyl pentapeptide involved in the formation of Gram-negative cross-linked peptidoglycan. *S*-1AEP is a slow onset inhibitor of the *S. enterica* D-alanine:D-alanine ligase, exhibiting a K_i value of 0.5 mM (*25*). *S*-1AEP is also a slow onset inhibitor of the *Streptococcus faecalis* alanine racemase (*26*). Thus, PhnO, by acetylating *S*-1AEP, would protect against the deleterious effects of *S*-1AEP as a result of the inhibition of these two key enzymes in peptidoglycan biosynthesis.

ACKNOWLEDGMENT

We thank Sophie Magnet (AECOM) for the generous donation of the *S. enterica* pET-28a(−):*phnO* construct. The authors thank Argyrides Argyrou for thoughtful discussions.

REFERENCES

1. Vershinina, O. A., and Znamenskaia, L. V. (2002) The Pho regulons of bacteria, *Mikrobiologiia 71*, 581−595.
2. Kononova, S. V., and Nesmeyanova, M. A. (2002) Phosphonates and their degradation by microorganisms, *Biochemistry (Moscow) 67*, 184−195.
3. Kennedy, K. E., and Thompson, G. A., Jr. (1970) Phosphonolipids: localization in surface membranes of *Tetrahymena*, *Science 168*, 989−991.
4. Conlin, C. A., Tan, S. L., Hu, H., and Segar, T. (2001) The apeE gene of *Salmonella enterica* serovar Typhimurium is induced by phosphate limitation and regulated by phoBR, *J. Bacteriol. 183*, 1784−1786.
5. Wanner, B. L. (1994) Molecular genetics of carbon−phosphorus bond cleavage in bacteria, *Biodegradation 5*, 175−184.
6. Metcalf, W. W., and Wanner, B. L. (1993) Evidence for a fourteen-gene, *phnC* to *phnP* locus for phosphonate metabolism in *Escherichia coli*, *Gene 129*, 27−32.
7. Jiang, W., Metcalf, W. W., Lee, K. S., and Wanner, B. L. (1995) Molecular cloning, mapping, and regulation of Pho regulon genes for phosphonate breakdown by the phosphonatase pathway of *Salmonella typhimurium LT2*, *J. Bacteriol. 177*, 6411−6421.
8. Wackett, L. P., Shames, S. L., Venditti, C. P., and Walsh, C. T. (1987) Bacterial carbon−phosphorus lyase: products, rates, and regulation of phosphonic and phosphinic acid metabolism, *J. Bacteriol. 169*, 710−717.
9. White, A. K., and Metcalf, W. W. (2004) Two C−P lyase operons in *Pseudomonas stutzeri* and their roles in the oxidation of phosphonates, phosphite, and hypophosphite, *J. Bacteriol. 186*, 4730−4739.
10. Kim, A. D., Baker, A. S., Dunaway-Mariano, D., Metcalf, W. W., Wanner, B. L., and Martin, B. M. (2002) The 2-aminoethylphosphonate-specific transaminase of the 2-aminoethylphosphonate degradation pathway, *J. Bacteriol. 184*, 4134−4140.
11. Metcalf, W. W., and Wanner, B. L. (1993) Mutational analysis of an *Escherichia coli* fourteen-gene operon for phosphonate degradation, using TnphoA′ elements, *J. Bacteriol. 175*, 3430−3442.
12. Metcalf, W. W., and Wanner, B. L. (1991) Involvement of the *Escherichia coli phn* (psiD) gene cluster in assimilation of phosphorus in the form of phosphonates, phosphite, Pi esters, and Pi, *J. Bacteriol. 173*, 587−600.
13. Kulakova, A. N., Kulakov, L. A., Akulenko, N. V., Ksenzenko, V. N., Hamilton, J. T., and Quinn, J. P. (2001) Structural and functional analysis of the phosphonoacetate hydrolase (*phnA*) gene region in *Pseudomonas fluorescens* 23F, *J. Bacteriol. 183*, 3268−3275.
14. Dumora, C., Marche, M., Doignon, F., Aigle, M., Cassaigne, A., and Crouzet, M. (1997) First characterization of the phosphonoacetaldehyde hydrolase gene of *Pseudomonas aeruginosa*, *Gene 197*, 405−412.
15. Baker, A. S., Ciocci, M. J., Metcalf, W. W., Kim, J., Babbitt, P. C., Wanner, B. L., Martin, B. M., and Dunaway-Mariano, D. (1998) Insights into the mechanism of catalysis by the P−C bond-cleaving enzyme phosphonoacetaldehyde hydrolase derived from gene sequence analysis and mutagenesis, *Biochemistry 37*, 9305−9315.
16. Olsen, D. B., Hepburn, T. W., Lee, S. L., Martin, B. M., Mariano, P. S., and Dunaway-Mariano, D. (1992) Investigation of the substrate binding and catalytic groups of the P−C bond cleaving enzyme, phosphonoacetaldehyde hydrolase, *Arch. Biochem. Biophys. 296*, 144−151.
17. Zhang, G., Morais, M. C., Dai, J., Zhang, W., Dunaway-Mariano, D., and Allen, K. N. (2004) Investigation of metal ion binding in phosphonoacetaldehyde hydrolase identifies sequence markers for metal-activated enzymes of the HAD enzyme superfamily, *Biochemistry 43*, 4990−4997.
18. Vetting, M. W., de Carvalho, L. P. S., Yu, M., Hegde, S. S., Magnet, S., Roderick, S. L., and Blanchard, J. S. (2005) Structure and functions of the GNAT superfamily of acetyltransferases, *Arch. Biochem. Biophys. 433*, 212−226.
19. Chase, J. F., Middleton, B., and Tubbs, P. K. (1966) A coenzyme A analogue, desulpho-coA; preparation and effects on various enzymes, *Biochem. Biophys. Res. Commun. 23*, 208−213.
20. Yan, Y., Harper, S., Speicher, D. W., and Marmorstein, R. (2002) The catalytic mechanism of the ESA1 histone acetyltransferase involves a self-acetylated intermediate, *Nat. Struct. Biol. 9*, 862−869.
21. Wozniak, M., Nicole, J., and Tridot, G. (1972) N°701—Complexes du cuivre (II) et des acides α-aminoalkylphosphoniques: correlation entre acidites, facteurs steriques et pouvoir complexant, *Bull. Soc. Chem. 11*, 4445−4452.
22. Song, B., Chen, D., Bastian, M., Martin, B. R., and Sigel, H. (1994) Metal-ion-coordination properties of a viral inhibitor, a pyrophosphate analogue, and a herbicide metabolite, a glycinate analogue: the solution properties of the potentially five-membered chelates derived from phosphonoformic acid and (aminoethyl)phosphonic acid, *Helv. Chem. Acta 77*, 1738−1756.
23. Draker, K. A., Northrop, D. B., and Wright, G. D. (2003) Kinetic mechanism of the GCN5-related chromosomal aminoglycoside acetyltransferase AAC(6′)-Ii from *Enterococcus faecium*: evidence of dimer subunit cooperativity, *Biochemistry 42*, 6565−6574.
24. Badet, B., Inagaki, K., Soda, K., and Walsh, C. T. (1986) Time-dependent inhibition of *Bacillus stearothermophilus* alanine racemase by (1-aminoethyl)phosphonate isomers by isomerization to noncovalent slowly dissociating enzyme-(1-aminoethyl)phosphonate complexes, *Biochemistry 25*, 3275−3282.
25. Duncan, K., and Walsh, C. T. (1988) ATP-dependent inactivation and slow binding inhibition of *Salmonella typhimurium* D-alanine:D-alanine ligase (ADP) by (aminoalkyl)phosphinate and aminophosphonate analogues of D-alanine, *Biochemistry 27*, 3709−3714.
26. Badet, B., and Walsh, C. (1985) Purification of an alanine racemase from *Streptococcus faecalis* and analysis of its inactivation by (1-aminoethyl)phosphonic acid enantiomers, *Biochemistry 24*, 1333−1341.

BI052297P